Effect of wave period on combined-flow bedforms: a flume experiment

T. Sekiguchi
Terrestrial Environment Research Center, University of Tsukuba, Japan

M. Yokokawa
Faculty of Information Science & Technology, Osaka Institute of Technology, Japan

ABSTRACT: Bedforms under combined flow with wave periods T = 1.5 and 1.0 s are examined through an experiment by using a recirculating flume. Three types of bedforms, *i.e.*, relatively symmetrical small ripples (SSR), asymmetrical small ripples (ASR), and asymmetrical large ripples (ALR), formed in the above order with increase in the unidirectional-flow component of the combined flow for T = 1.5 s. For T = 1.0 s, the ASR developed with a larger unidirectional-flow component as compared to those developed for T = 1.5 s, and the ALR did not occur despite the large unidirectional-flow component in this test. The experimental results of this test for T = 1.5 s showed good agreement with the phase diagram for T = 10.5 s in the previous study; this impliesthat the effects of wave period on the shape of bedforms is significant between T = 1.0 sec and 1.5 s, and may be minor when $T \geq 1.5$ s.

1 INTRODUCTION

Combined flow, which commonly refers to a combination of unidirectional and wave-induced oscillatory flow that is omnipresent in the natural environments (e.g., Dumas et al., 2005), generates bedforms on a sandy bottom. Combined-flow bedforms abundantly exist in coastal and lake environments, and the ancient combined-flow bedforms exist in stratigraphical records. Because bed roughness affects the dynamics of the bottom boundary layer and sediment transport, the relationship between the sizes of the bedforms and hydraulic conditions has been intensely investigated by field (e.g., Li et al., 1996; Li & Amos, 1998) and laboratory studies (e.g., Tanaka & Dang, 1996; Khelifa & Ouellet, 2000; Yovanni et al., 2006).

From the geological point of view, the shapes of bedforms as well as their size are important in order to interpret the ancient sedimentary environments under which bedforms in strata formed. Through experiments, Arnott & Southard (1990), Yokokawa (1995), and Dumas et al. (2005) have classified combined-flow bedforms based on their shape and size and have proposed phase diagrams of the bedforms. However, such phase diagrams of combined-flow bedforms have been proposed only for limited hydraulic conditions.

This study presents the results of an experiment on combined-flow bedforms and focuses on their shapes. A bedform phase diagram is proposed, and comparisons between the previous phase diagrams are made for the different wave period.

2 EXPERIMENT

A recirculating flume of length, breadth, and depth 12 m, 0.2 m, and 0.5 m, respectively, which belongs to the Department of Environmental Systems Science, Faculty of Engineering, Doshisya University, was employed in this test (Fig. 1). The flume has a

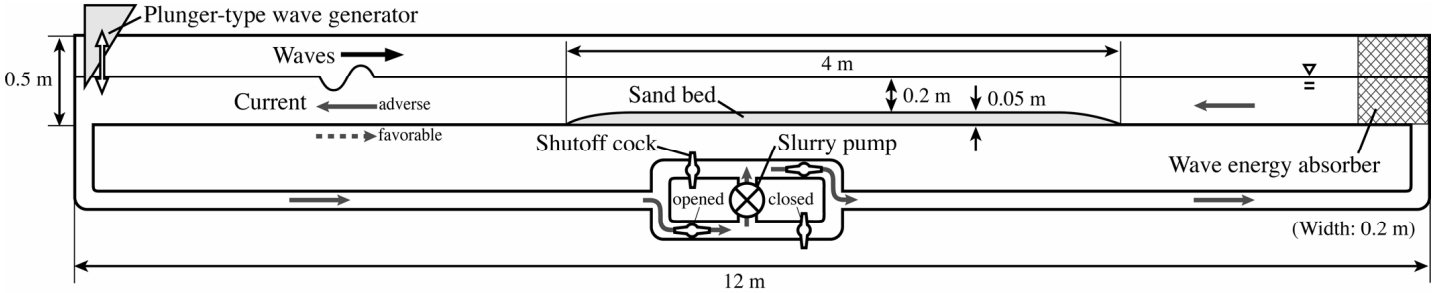

Figure 1. Recirculating flume used in this test.

plunger-type wave generator at one end, and a wave absorber at the other end in order to reduce the reflecting wave energy. A plumbing system in the flume enable to control the current direction, which is generated by a slurry pump integrated into the system. Therefore, the flume can generate two types of combined flow with different combinations of directions of waves and current: (1) "favorable" combined flow, in which the waves and current travel along the same direction and (2) "adverse" combined flow, in which the directions of the waves and current are opposite. Here, the terms "onshore" and "offshore" represent the directions of wave propagation, and "upstream" and "downstream" indicate the directions of current. In contrast to the purely symmetrical oscillatory flow in oscillatory-flow tunnel, wave-induced oscillatory flow is commonly skewed; the onshore flow possesses larger velocity and shorter duration as compared to the offshore flow (e.g., Komar, 1998). The examination of bedforms under both favorable and adverse combined-flow conditions will show the effects of the asymmetry in wave-induced flow.

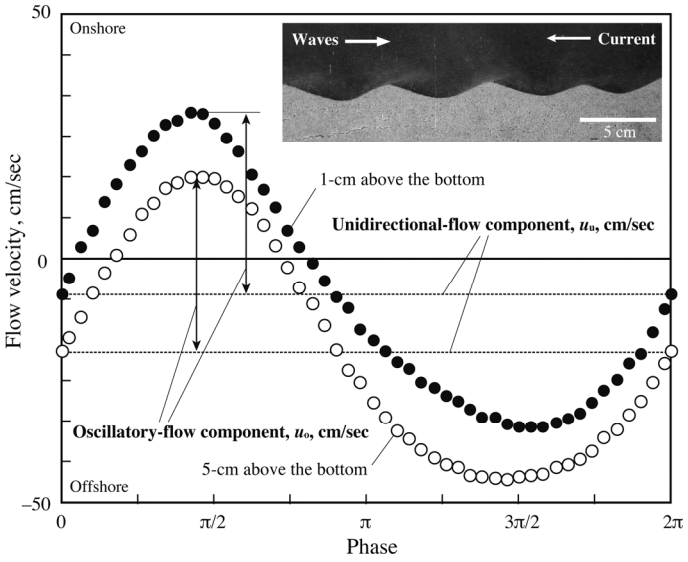

Figure 2. Relationship between the near-bottom flow field, intermediate flow field, and ripple geometry.

This study examines the bedforms, which develop from a flat horizontal sand bed under various combined-flow conditions through 67 experimental runs. The length, width, and height of the sand bed are 4 m, 0.2 m, and 0.05 m, respectively. The bed material is well-sorted quartz sand with a median grain diameter D = 0.2 mm. The hydraulic conditions in this test are as follows: h = 20 cm, T = 1.5 and 1.0 sec, $u_o \leq 55$ cm/s, and -45 cm/s $\leq u_u \leq 34$ cm/s where h is the water depth above the bed; T, the wave period; and u_o and u_u, the oscillator-flow and unidirectional-flow velocity components of the combined flow, respectively (Fig. 2). The positive and negative of u_u values indicate the current direction relative to the wave direction: the positive value indicates the favorable (onshore) direction, and the negative value indicates the adverse (offshore) direction. Here, the absolute value of u_u will be represented as $|u_u|$.

The u_o and u_u values were obtained by using flow velocity data at a distance of 1 cm above the sand bed, which are measured by an acoustic Doppler velocimeter. This is because our preliminary experiment showed that the degree of ripple asymmetry agreed better with the degree of asymmetry in the near-bottom flow field at a distance of 1 cm above the bed as compared to that in the intermediate flow field at a distance of 5 cm above the bed (Fig. 2). The development processes of bedforms are recorded on a digital video camera, and their digital photographs are taken at certain intervals of time.

3 RESULTS AND DISCUSSION

The resulting bedforms showed significant variation in their shapes and sizes, and were categorized into three types based on the degrees of ripple asymmetry, shape of ripple crest, and ripple wavelength, as follows: (1) relatively symmetrical small ripples (Fig. 3a), (2) asymmetrical small ripples (Fig. 3b) and (3) asymmetrical large ripples (Fig. 3c). The "asymmetrical ripples" indicate ripples with ripple symmetry index ($RSI = b/a$ where a and b denote horizontal lengths of lee and stoss sides, respectively; Fig. 4) greater than 2 (Dumas et al., 2005), and "large ripples" indicated those with $\lambda \geq 30$ cm, where λ denotes the ripple wavelength.

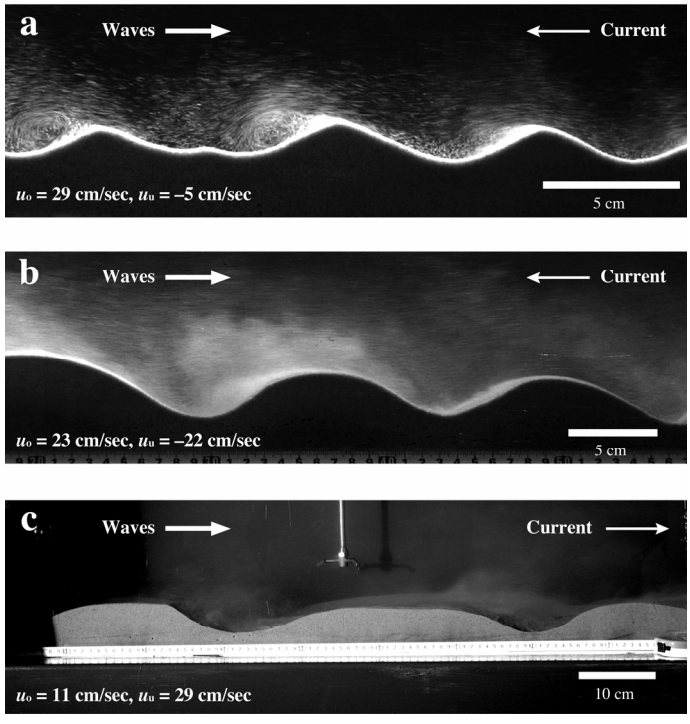

Figure 3. Profiles of the combined-flow bedforms developed in this test: (a) relatively symmetrical small ripples, (b) asymmetrical small ripples, and (c) asymmetrical large ripples.

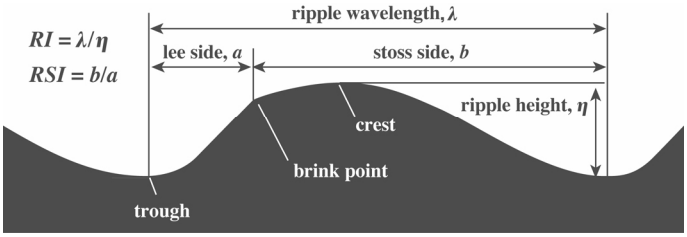

Figure 4. Terminology used to describe the ripple morphology.

It should be noted that the bedforms were not always in the equilibrium state even at the end of the experimental runs. Because of the limited sizes of the sand bed and flume, the durations of the experimental runs were not sufficiently long for the development of the equilibrium state of the bedforms particularly for cases with current-dominant conditions (e.g., Baas, 1999). Therefore, the relationship between the sizes of the bedforms and the near-bottom-flow conditions will not be examined in this test.

However it is worthwhile to describe their characteristics because bedforms in the natural environments are not always in the equilibrium state (e.g., Traykovski et al., 1999). The characteristics and formative conditions of the three types of bedforms will be described bellow.

3.1 *Characteristics of bedforms*

Relatively symmetrical small ripples (Fig. 3a; hereafter called as SSR), are similar to ripples developed under wave-induced oscillatory flow alone. The SSR are two-dimensional ripples, and their profile is relatively symmetrical with $1 \leq RSI \leq 2$. Their crest and brink point are undivided, and their crest is sharp and angular. The trough of SSR shows a rounded profile. The Ripple Index ($RI = \eta/\lambda$, where η denotes the ripple height; Fig. 3) generally fall in the range $4 \leq RI \leq 10$. In this test, this type of ripples has wavelength $\lambda \leq 10$ cm. SSR form under the relatively symmetrical near-bottom flow field, which generates the vortices over both lee and stoss sides. The vortices entrap sediment grains, and suspend them over the bed. The near-bottom suspended sediment clouds are transported along both the upstream and the downstream directions due to the wave-induced to-and-fro flows, and the combined-flow ripples form with a relatively symmetrical profile. However, as described before, the intermediate combined-flow field possesses a larger unidirectional-flow component as compared to the near-bottom combined-flow field; thus the suspended sediment grains in the intermediate layer travel almost only along the downstream direction.

Asymmetrical small ripples (ASR; Fig. 3b) are generally two-dimensional ripples; however they are more or less irregular. The crest of this type of ripples with $RSI \geq 2$ is not always equal to the brink point; the crest of ASR is generally rounded. The *RI*-value is commonly in the range of $4 \leq RI \leq 8$, and the wavelength of this type of ripple is smaller than 30 cm. Combined flows with the moderate $|u_u|$ values form this type of ripple. The vortices are generated only over the lee sides. Because the vortices excavate sediment grains in the trough area, the trough is rounded. The sediment grains entrapped in the vortices are transported in the mode of suspension almost only downstream even in the near-bottom layer.

Asymmetrical large ripples (ALR; Fig. 3c) are two- or three-dimensional ripples, and with $RSI \geq 3$ and $RI \geq 8$. The crest and brink point of these ripples tend to be separated. The wavelength of ALR is greater than 30 cm but less than 100 cm; this may be due to the limited duration of the experimental runs. Combined flow with large $|u_u|$ values form this type of ripple. The sediment grains are suspended due to strong vortices, which are generated only over lee sides, and the suspended clouds are transported only downstream.

3.2 *Formative conditions of three types of ripples*

The conditions for the development of the three types of ripples and for the formation of no ripples are plotted on the u_u–u_o planes (Arnott & Southard, 1990; Yokokawa, 1995; Dumas et al., 2005) for T = 1.5 s (Fig. 5a) and 1.0 s (Fig. 5b). Yokokawa's (1995) data for T = 1.0 s and 1.25 s are also plotted on the u_u–u_o plane for T = 1.0 s (Fig. 5b): Yokokawa's (1995) wave-dominated and current dominated combined-flow ripples (abraded as W.D. CFR and C.D. CFR in Fig. 5, respectively) are equivalent to the SSR and ASR in this study, respectively.

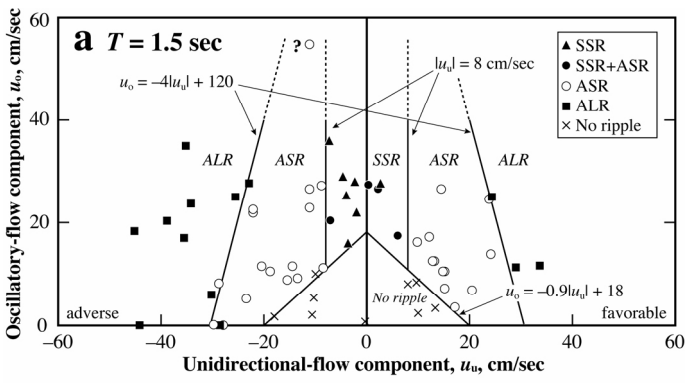

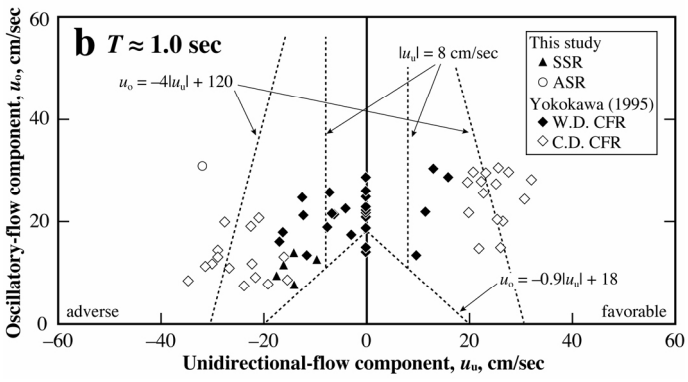

Figure 5. Combined-flow phase diagram with the unidirectional-flow component and oscillatory flow component as axes for (a) T = 1.5 s, and for (b) T = 1.0 s.

The boundaries between the SSR, ASR, and ALR disagree with the phase diagrams for T = 1.5 s and 1.0 s (Fig. 5). The combined-flow ripples form when $u_o \geq -0.8|u_u| + 16$. For T = 1.5 s, the SSR develop when $|u_u| \leq 8$ cm/s; ASR, when $|u_u| \geq 8$ cm/s and $u_o \leq -4|u_u| + 120$; and ALR, when $u_o \geq -4|u_u| + 120$ (Fig. 4a). When $T \approx 1.0$ s, the SSR develop when $|u_u| \leq 8$ cm/s, and ASR, when 8 cm/s $\leq |u_u| \leq 35$ cm/s. ALR are not observed in this test (Fig. 5b).

These results show that the positive and negative u_u values do not significantly affect the developments of the combined-flow bedforms (Fig. 5). Thus, the effect of the asymmetry in wave-induced oscillatory-flow component on the formation of the combined-flow bedforms appears negligible, at least when $T \leq 1.5$ s and D = 0.2 mm.

The comparison between our data for T = 1.5 s and Dumas et al.'s (2005) phase diagram for T = 10.5 s and D = 0.22 mm shows good agreement (Fig. 6). This implies that the effects of wave period on the shape of bedforms may be minor when $T \geq 1.5$ s; further experiments with 2 s $\leq T \leq$ 10 s are expected.

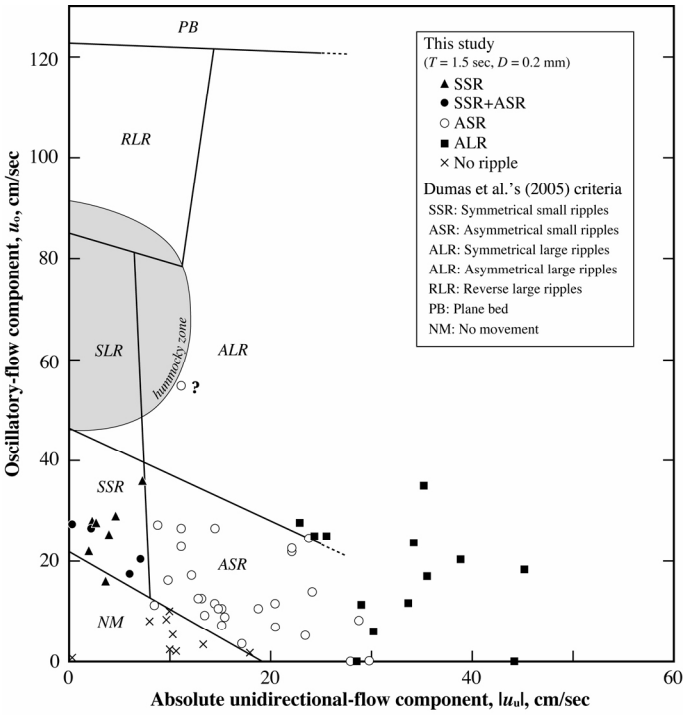

Figure 6. Comparison between the formative conditions of the combined-flow bedforms in this test and Dumas et al.'s (2005) phase diagram for T = 10.5 s and D = 0.22 mm.

4 CONCLUSION

This flume experiment examined combined-flow bedforms for T = 1.0 s and 1.5 s and D = 0.2 mm. Three types of bedforms, SSR, ASR, and ALR, formed in the above order with increase in the $|u_u|$ values for T = 1.5 s; however, ALR did not form in this test for T = 1.0 s. Phase diagrams for T = 1.0 sec and for T = 1.5 sec disagreed with each other, but the latter is consistent with Dumas et al.'s (2005) phase diagram for T = 10.5 s.

5 ACKNOWLEDGEMENT

This study is partially supported by the Grant-in-Aid for Young Scientists (B) 19740309, the Ministry of Education, Culture, Sports, Science and Technology, Japan.

REFERENCES

Arnott, R.W.C. & Southard, J.B. 1990. Exploratory flow-duct experiments on combined-flow bed configurations, and some implications for interpreting storm-event stratification. *Journal of Sedimentary Petrology* 60: 211–219.

Baas J. 1999. An empirical model for the development and equilibrium morphology of current ripples in fine sand. *Sedimentology* 46: 123–138.

Cataño-Lopera, Y.A. & García, M.H. 2006. Geometry and migration characteristics of bedforms under waves and currents Part 2: Ripples superimposed on sandwaves. *Coastal Engineering* 53: 781–792.

Dumas, S., Arnott, R.W.C. & Southard, J.B. 2005. Experiments of oscillatory-flow and combined-flow bed forms: implications for interpreting parts of the shallow-marine sedimentary record. *Journal of Sedimentary Research* 75(3): 501–513.

Khelifa, A. & Ouellet, Y. 2000. Predictions of sand ripple geometry under waves and currents. *Journal of Waterway Port Coastal and Ocean Engineering*, ASCE, 126 (1): 14–22.

Komar, P.D. 1998. Beach Processes and Sedimentation. Prentice Hall: Upper Saddle River.

Li, M.Z., Wright, L.D. & Amos, C.L., 1996. Predicting ripple roughness and sand resuspension under combined flows in a shoreface environment. *Marine Geology* 130: 139–161.

Li, M.Z. & Amos, C.L. 1998. Predicting ripple geometry and bed roughness under combined waves and currents in a continental shelf environment. *Continental Shelf Research* 18: 941–970.

Tanaka, H. & Dang, V.T. 1996. Geometry of sand ripples due to combined wave–current flows. Journal of Waterway Port Coastal and Ocean Engineering, ASCE, 122 (6): 298–300.

Traykovski, P., Hay, A.E., Irish, J.D. & Lynch, J.F. 1999. Geometry, migration, and evolution of wave orbital ripples at LEO-15. *Journal of Geophysical Research* 104C: 1505–1524.

Yokokawa, M. 1995. Combined-flow ripples: genetic experiments and applications of geologic records, *in* Memoirs from the Faculty of Science: Kyushu University, Series D, Earth and Planetary Sciences, v. 29, no. 1, Fukkuoka, Japan, 38p.